Laboratory Animals published by the US National Institute of Health (NIH Publication No. 85-23, revised 1996).

2.4. Western blot analysis for eNOS and iNOS

The levels of eNOS and iNOS expression in vessels were determined by Western blot analysis [16]. Band intensities were analyzed densitometrically by the National Institute of Health IMAGE program.

2.5. Vascular response

Seven days after gene transfer, the rabbits ($n=6$ each group) were anesthetized with pentobarbital (50 mg/kg

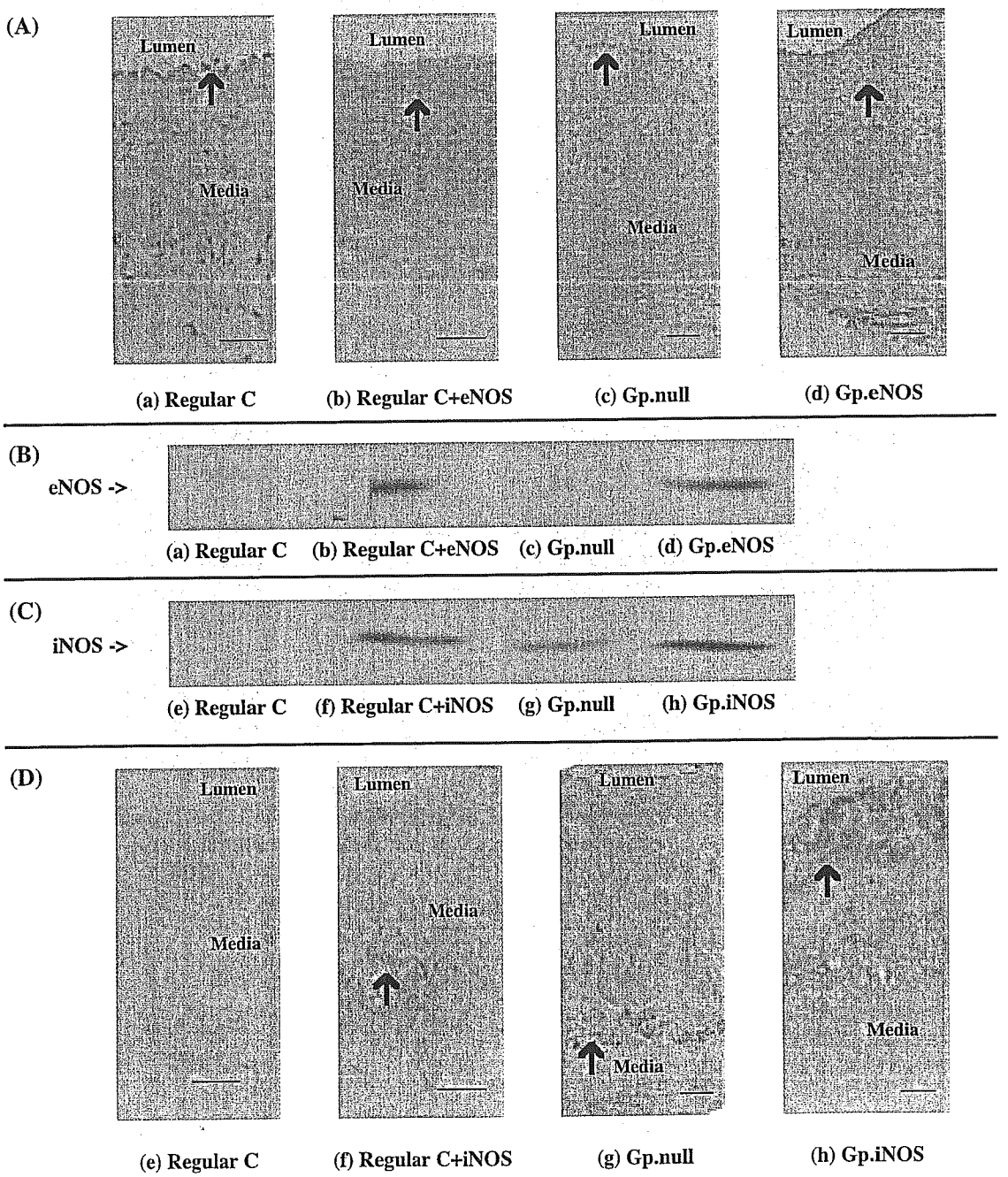

Fig. 1. Upper: localization of eNOS expression by immunostaining (arrows). Arteries from Gp regular c (a), gene transfer of eNOS to Gp regular c (b), Gp null (c), and Gp eNOS (d) were stained. Middle: Western blot analysis for eNOS. Lane 1: control (aorta from Gp regular c); Lane 2: aorta from Gp regular c transfected with eNOS; Lane 3: atherosclerotic control aorta from Gp null; Lane 4: aorta from Gp eNOS (transfected with eNOS to atherosclerotic artery). Western blot analysis for iNOS (f). Lane 1: control (aorta from Gp regular c); Lane 2: aorta from Gp regular c transfected with iNOS. Lane 3: atherosclerotic control (aorta from Gp null), Lane 4: aorta from Gp iNOS (Ad.iNOS). Lower: localization of iNOS expression by immunostaining (arrows). The artery from Gp regular c (e), gene transfer of iNOS to Gp regular c (f), Gp null (g), and Gp iNOS (h) were stained. The scale bar represents 50 μm.

intravenously) and sacrificed by exsanguination. Vascular responses were investigated as described previously [15]. Briefly, aortae were cut into 2-mm-wide transverse rings. The rings were stretched to their optimal force, which was predetermined by a force of 122 mM KCl, and mounted in chambers filled with Krebs'–Henseleit solution at 37 °C. The response of endothelium-intact rings to ACh and that of endothelium-denuded rings to NTG were determined under submaximal contraction induced by PGF2α (2.6×10^{-6} M) [17]. Tone-related basal NO-dependent contractile responses to L-NMA were assessed under moderate tone (about 40% contraction by KCl) induced by PGF2α (0.8×10^{-6} M) [17].

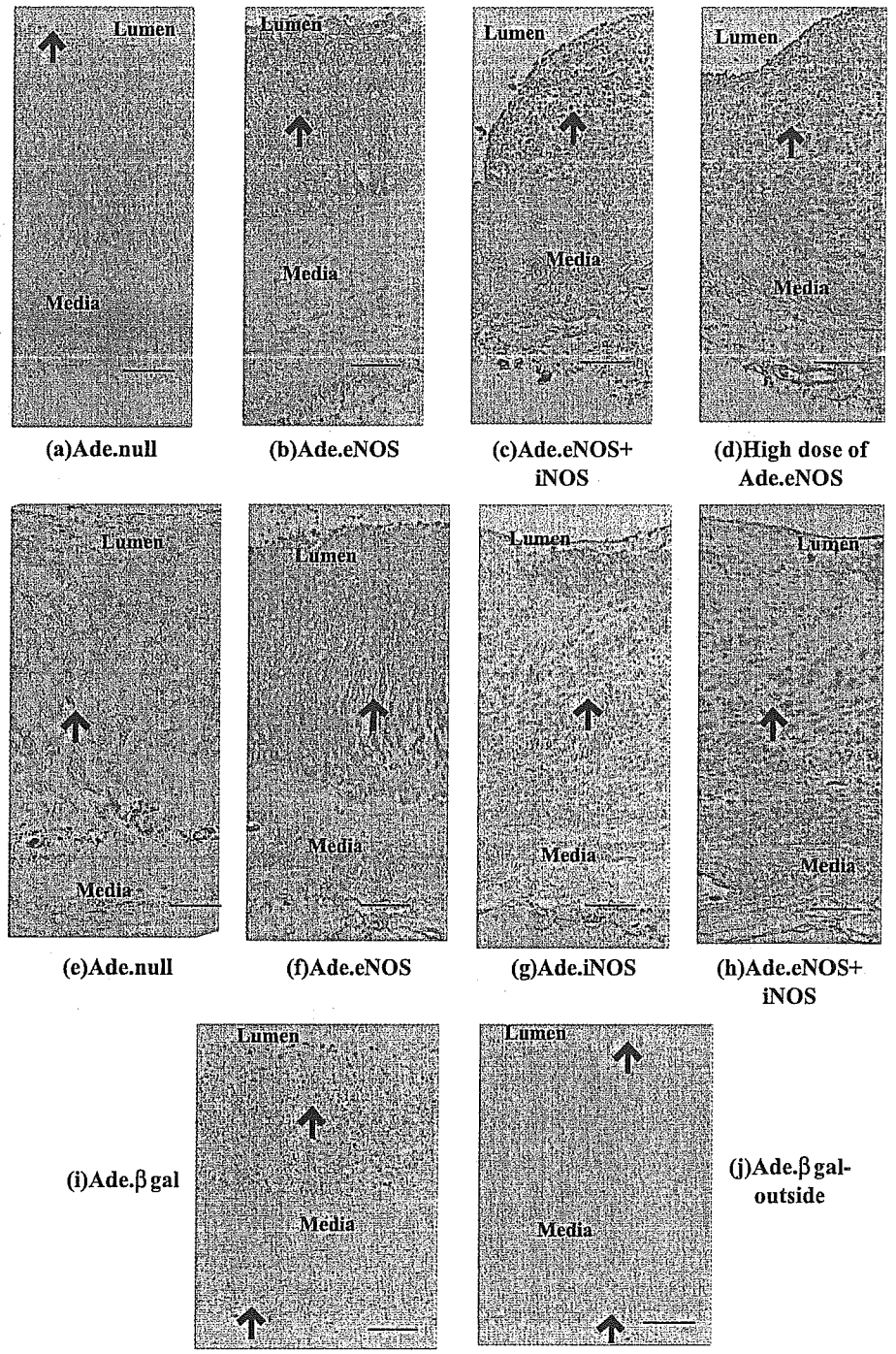

Fig. 2. Upper: localization of eNOS expression by immunostaining. Arteries infected with: (a) Ad.eNOS (Gp eNOS); (b) Ad.eNOS (Gp eNOS); (c) Ad.eNOS plus Ad.iNOS (Gp e+i); and (d) a high dose of Ad.eNOS (Gp heNOS) were stained. Original magnification, × 150. Middle: localization of iNOS (e, f, g and h) expression by immunostaining. Arteries infected with: (e) Ad.null; (f) Ad.eNOS; (g) Ad.iNOS; (h) Ad.eNOS+iNOS. Original magnification, × 100. Lower: localization of β gal expression by immunostaining. The section from the gene transfer site with Ad. β-gal (Gp β-gal) (i). The section from the site outside the gene transfer site of Ad. β-gal (Gp β-gal) (j). Original magnification, × 150. The scale bar represents 50 μm.

Table 1
Lipid and NO related profile

	Tissue			Tissue		Tissue		
	T. Chol. (mg/dl)	T.G. (mg/dl)	HDL-C (mg/dl)	T. Chol. (mg/wet g)	E. Chol. (mg/wet g)	cGMP (pmol/wet g)	NOx (nM/wet g/24 h)	$O2^-$ release (μM)
Gp cont	1771.0 ± 210.3	66.9 ± 8.9	67.4 ± 7.3	5.62 ± 0.26	3.18 ± 0.42	3.04 ± 0.28	4.6 ± 0.7	0.31 ± 0.06
Gp null	1826.1 ± 171.3	61.8 ± 8.2	62.0 ± 4.0	5.45 ± 0.16	3.05 ± 0.31	2.63 ± 0.21	4.4 ± 0.6	0.34 ± 0.04
Gp eNOS	1690.5 ± 170.4	62.4 ± 8.5	63.1 ± 5.0	4.78* ± 0.41	2.49* ± 0.41	5.95* ± 0.77	8.1* ± 2.5	0.25* ± 0.04
Gp iNOS	1804.7 ± 183.3	56.2 ± 4.9	59.5 ± 5.7	6.09 ± 0.38	3.31 ± 0.58	3.03 ± 0.45	5.1 ± 1.8	0.43* ± 0.05
Gp e+i	1725.0 ± 110.7	52.9 ± 3.7	52.0 ± 2.7	6.67 ± 0.57	3.47 ± 1.35	3.53 ± 0.17	5.6 ± 1.2	0.45* ± 0.06
Gp heNOS	1712.5 ± 191.4	59.4 ± 9.8	51.1 ± 7.2	4.69* ± 0.51	2.53* ± 0.42	5.81* ± 0.71	9.1* ± 2.1	0.27* ± 0.04
Gp regular c	84.1 ± 12.3	39.1 ± 6.9	49.6 ± 7.7	1.02 ± 0.18	N.D.	3.33 ± 0.75	4.9 ± 1.1	0.19 ± 0.04

T. Chol.: total cholesterol, T.G.: triglyceride, T.P.: total protein, g.t.: gene transfer, N.D.: not detected.
*$P<0.05$ vs. Gp null.

In some studies, indomethacin (5×10^{-6} M) was added to the chambers to rule out the contribution of prostanoids.

2.6. Measurement of lipids

Serum lipids were measured by enzymatic assays [18].

2.7. Measurement of cyclic GMP (cGMP)

The basal concentrations of cGMP in aortae were determined by an enzyme-linked immunoassay (Amersham, Buckinghamshire, UK) [19]. Four rings were used from each rabbit.

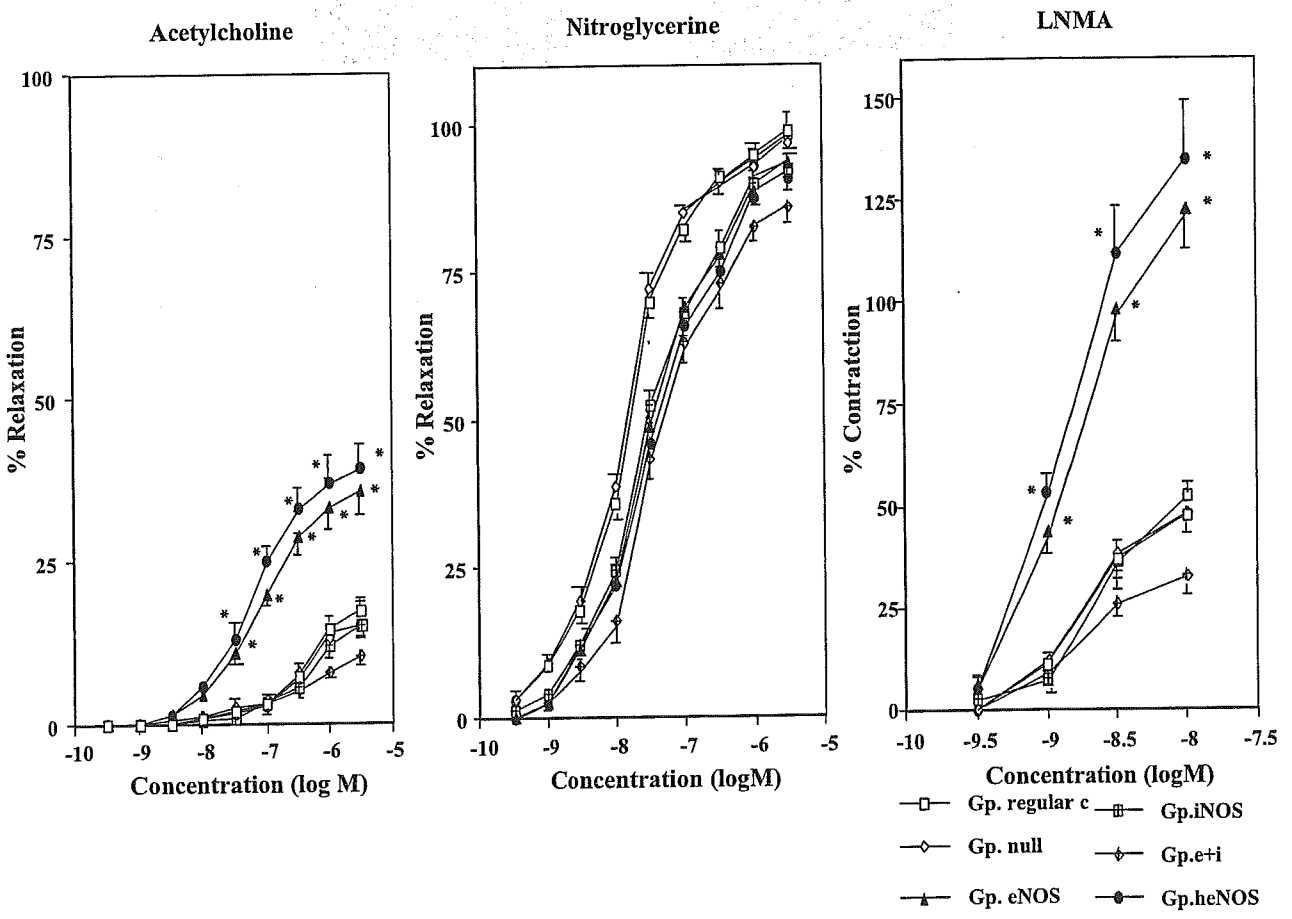

Fig. 3. Cumulative concentration–response curves to each of the agonists in the abdominal aortae of seven groups, which were precontracted by prostaglandin F2α: Gp cont: no treatment; Gp null: Ad.null; Gp eNOS: Ad.eNOS; Gp iNOS: Ad.iNOS; Gp e+i: Ad.eNOS plus Ad.iNOS; Gp heNOS: high amount of Ad.eNOS. Left: cumulative concentration–response curves to acetylcholine. Middle: cumulative concentration–response curves to nitroglycerin. Right: cumulative concentration–response curves to L-NMA; NOS inhibitor. % indicates the percentage vs. the magnitude of the contraction level by PGF2α. *$P<0.05$ vs. Gp null.

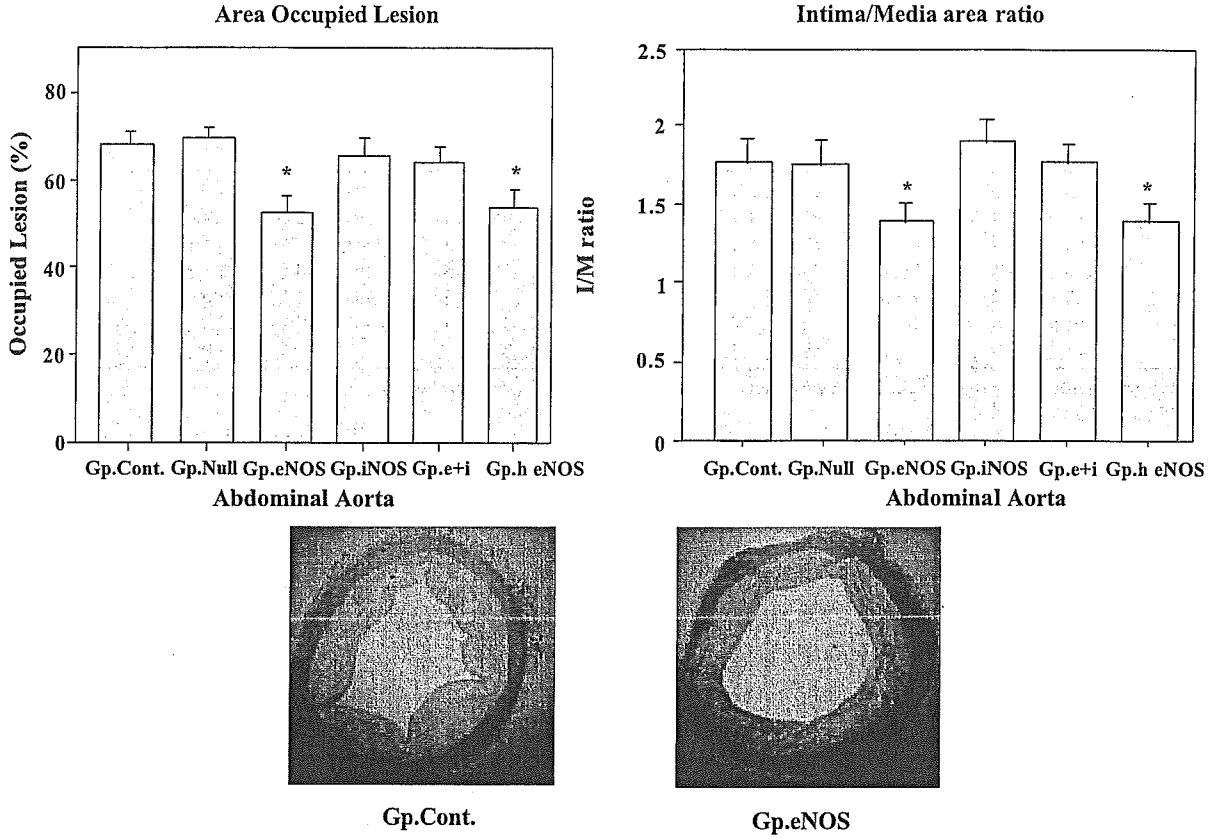

Fig. 4. Histological evaluation of the atherosclerotic area of the aorta as indicated by the mean lesion area (% occupied lesion, left), and the intima/medial ratio (I/M ratio, Right). Gp cont: no treatment; Gp null: Ad.null; Gp eNOS: Ad.eNOS; Gp iNOS: Ad.iNOS; Gp e+i: Ad.eNOS plus Ad.iNOS; Gp heNOS: high amount of Ad.eNOS. Lower: a section stained with H.E. from Gp cont and Gp eNOS. Original magnification, × 40. The scale bar represents 200 μm.

2.8. Measurement of nitrite and nitrate (NO_2^-/NO_3^-) and detection of aortic superoxide generation

NOx (sum of nitrite and nitrate, NO_2^-/NO_3^-) was measured in medium containing 2 mm-wide of abdominal aorta from each group in 24 well culture dishes (medium: 100 μl of phenol red free DMEM + 10% fetal calf serum, cultured for 24 h). An NO detector-HPLC system (ENO10; Eicom, Kyoto, Japan) was used as previously reported [20]. Formation of O_2^- was assayed by measuring the intensity of chemiluminescence probes at physiological pH (7.4). Its signal was detected by a luminescence reader (BLR-201; Aloka, Tokyo). The O_2^- generation signal was defined as the inhibitory signal by superoxide dismutase (SOD, 100 U/ml).

2.9. Histological evaluation of atherosclerosis and assays for tissue

Cross sections of the aorta adjacent to the segments of vascular responses were examined [21]. The contours of the lumen and the internal elastic lamina (IEL) were traced. The area occupied by lesions was defined as the ratio of the area bounded by the lumen and IEL (atherosclerotic area) to the area bounded by the IEL (mean of six sections for one vessel). The intima/media ratio was also measured. A 0.8-cm-long segment of the gene-transferred portion was homogenized, and lipids were extracted to measure the cholesterol level [18].

2.10. Immunohistochemical study

This study was performed as described previously [22]. Tissues were sectioned into 5-mm-thick slices. Primary monoclonal antibodies (macrophages, smooth muscle cells, nitrotyrosine, MMP-1, or β galactosidase, each one × 250) were applied. Sections were incubated with biotinylated immunoglobulin and incubated with horseradish peroxidase-labeled avidin solution. DNA nick-end labeling of tissue sections (TUNEL staining) was performed as described previously [22]. Negative

Fig. 5. The representative immunohistochemical staining of abdominal aortae. Upper: a section stained with a monoclonal antibody against macrophages (arrow) from (a) Gp null: Ad.null; (b) Gp eNOS: Ad.eNOS; (c) Gp iNOS: Ad.iNOS; and (d) Gp e+i: Ad.eNOS plus Ad.iNOS. Original magnification, × 150. Middle upper: a section stained with a monoclonal antibody against nitrotyrosine (arrow): the marker of $ONOO^-$ from (e) Gp null, (f) Gp eNOS, (g) Gp iNOS, and (h) Gp e+i. Original magnification, × 150. Middle lower: a section stained with a monoclonal antibody against the marker of smooth muscle cell actin (arrow) from (i) Gp null, (j) Gp eNOS, (k) Gp iNOS, and (l) Gp e+i. Original magnification, × 100. Lumen: luminal area; media: media. The scale bar represents 50 μm. Lower: % area occupied by macrophages, nitrotyrosine and smooth muscle cells in atherosclerotic plaque was evaluated by immunohistochemistry (each group, $n = 8$).

controls included substitution of primary antibody with irrelevant antibodies. Each slide was scored for the presence of cells that were positive for each type of antibody, and was statistically analyzed as described in our previous report [6]. Five pieces of aortae were prepared from each rabbit.

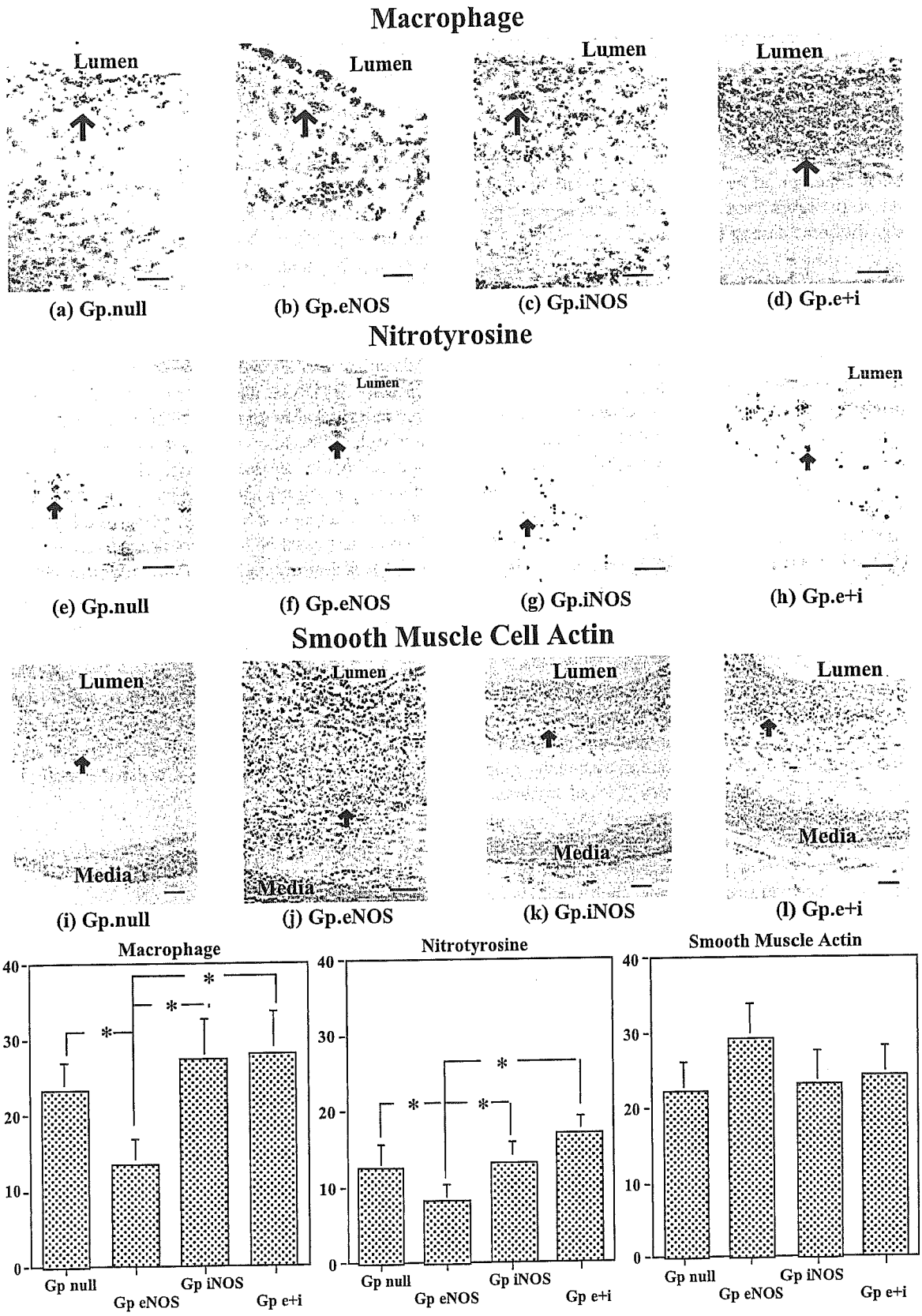

2.11. Statistical analysis

Data are presented as the means ± S.E.M. Student's *t*-test was used for determination of statistical significance, and Kruskal–Wallis one-way ANOVA was used for multiple comparisons. Values of $p < 0.05$ were considered to indicate statistical significance.

3. Results

All rabbits appeared to be healthy throughout the study period, and body weight and serum total protein were not significantly different among the groups.

3.1. Transgene expression in severe atherosclerotic aortae

Immunohistochemical staining of each NOS gene showed that the gene transfers were successful. Staining of intrinsic eNOS and iNOS was apparent in vessels from the Gp cont. However, only eNOS was observed in vessels from the Gp regular cont (Fig. 1). In the case of vessels treated with Ad.eNOS (Gp eNOS, Gp e+i and Gp heNOS), positive staining for eNOS was observed in a region of the endothelium, throughout the entire subintimal area, and slightly in the media and adventitial area (Fig. 2). In vessels treated with Ad.iNOS (Gp iNOS and Gp e+i), positive staining for iNOS was observed in part of the atheromatic area, especially around the necrotic core, and slightly in the endothelium and adventitial area (Fig. 2). The levels of eNOS and iNOS in the Gp e+i seemed to be almost the same as those in Gp eNOS and Gp iNOS. Even transfection of cells with a large amount of Ad.eNOS resulted in only a slight increase of eNOS expression (Fig. 2). In an additional experiment, the level of eNOS in the Ad.eNOS plus Ad.null treatment group and that of iNOS in the Ad.iNOS plus Ad.null treatment group were almost identical to those in the Gp eNOS and Gp iNOS, respectively (data not shown). Vessels treated with Ad.β galactosidase showed pronounced β galactosidase staining in the atheromatic regions, and slight staining in the adventitia, media, and endothelium (Fig. 2). However, the part of vessels outside of Ad. β galactosidase infection showed little β galactosidase staining (Fig. 2).

3.2. Western blot analysis for eNOS and iNOS

Expression of eNOS was confirmed in aortae of all groups, whether atherosclerosis was induced or not. Pronounced expression of eNOS was confirmed in aortae of the Ad.eNOS transfection groups (5.7 ± 1.6 times staining compared to that of the regular control group). Slight expression of iNOS was detected in aortae from groups in which advanced atherosclerosis was induced. Pronounced iNOS expression was detected in arteries treated with Ad.iNOS (Fig. 1). The amount of iNOS in Ad.iNOS-transduced arteries (Gp iNOS) was also comparable with that of eNOS in Gp eNOS. Even transfection of cells with a large amount of Ad.eNOS produced only a slight increase of eNOS expression (2.1 ± 0.4 times staining compared to that of Gp eNOS).

3.3. Blood chemistry

There were no significant differences in serum lipid levels (Table 1).

3.4. Vascular responses

Contraction by PGF2α in the Ad.eNOS-transfected groups (Gp eNOS, 1.9 ± 0.2 g; Gp heNOS, 1.8 ± 0.2 g) was slightly smaller than that of the other groups (2.2 ± 0.2, 2.2 ± 0.1, 2.0 ± 0.3 and 2.3 ± 0.3 g in the Gps cont, null, iNO, and e+i). Balloon injury and atherogenic diet diminished the ACh-induced relaxation in the aortae (Fig. 3). Relaxation was almost eliminated in the aorta of Gp cont, Gp null, Gp iNOS, and Gp e+i animals. Ad.eNOS transfection remarkably improved EDR (Fig. 3). The EDR levels in vessels from Gp e+n and Gp i+n were almost the same as those in vessels from Gp eNOS and Gp iNOS (data not shown). No significant difference was observed in NTG-induced relaxation among the aortae of all groups (Fig. 3). Tone-related basal NO-dependent contraction induced by L-NMA was highest in the aortae from Gp eNOS and Gp heNOS (Fig. 3). In an additional experiment, the contraction was also increased in the aortae from the Ad.eNOS plus Ad.null group, but was not increased in the group treated with Ad.iNOS plus Ad.null (data not shown). This finding indicates that the aortae from Gp eNOS, Gp heNOS, and the Ad.eNOS plus Ad.null group released larger amounts of tone-related basal NO than the vessels of the other groups. Preincubation with indomethacin did not affect EDR (data not shown).

3.5. Histological evaluation of atherosclerosis and aortic cholesterol content

Ad.eNOS regressed the atherosclerotic lesions in the abdominal aorta; however, transfection with a large amount of Ad.eNOS (Gp heNOS) resulted in only a slight increase in regression relative to that in Gp eNOS (Fig. 4). In an additional experiment, the total areas of lesions in the aortae of the Ad.eNOS plus Ad.null group or Ad.iNOS plus Ad.null group were almost identical to that of Gp eNOS or Gp iNOS, respectively. Total and esterified cholesterol content in vessels exhibited the same tendency as the atherosclerotic areas (Table 1).

3.6. Measurement of cyclic GMP

The concentrations of cGMP in aortic tissues from Gp eNOS and Gp heNOS increased significantly compared to other groups (Table 1).

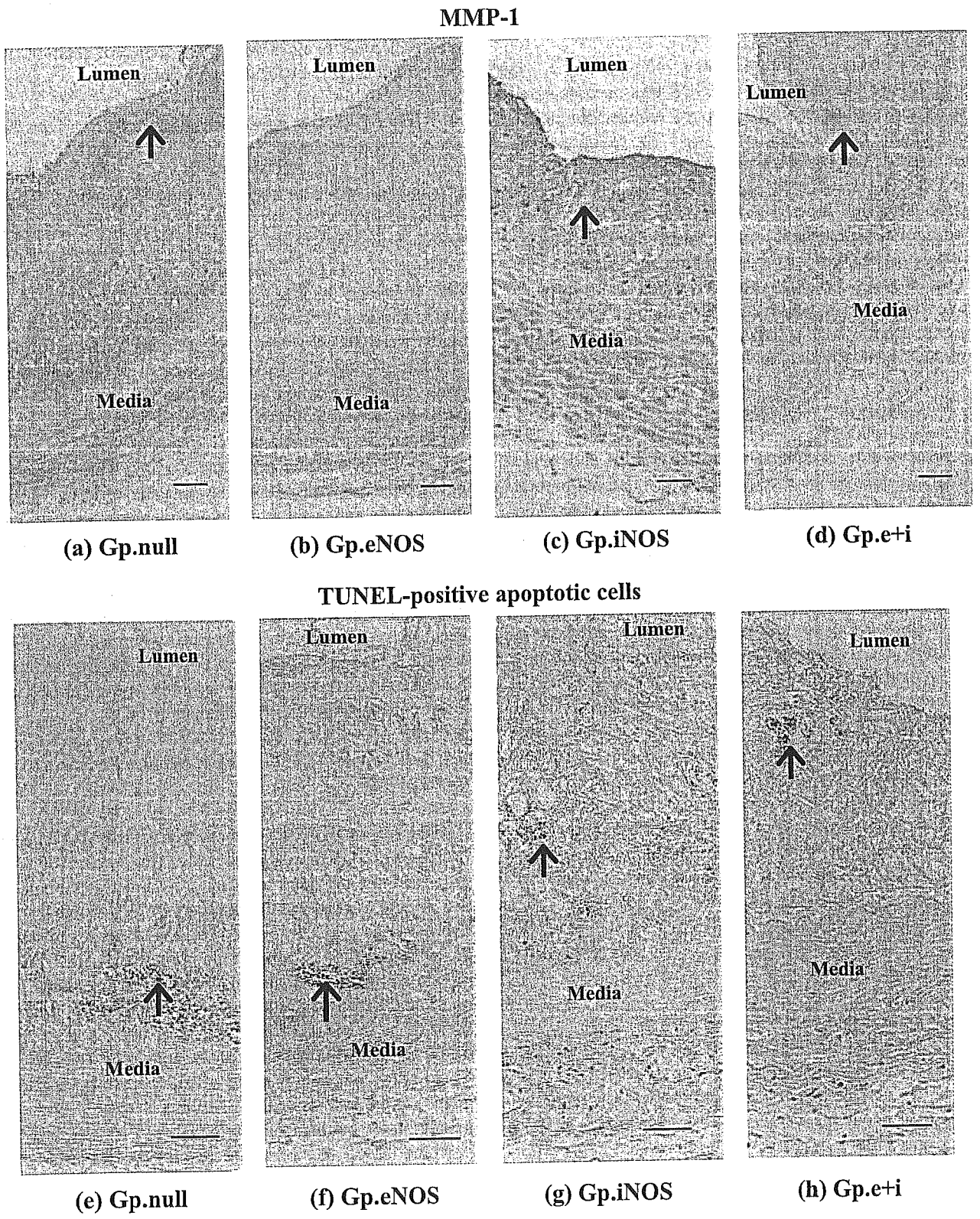

Fig. 6. Upper: expression of MMP-1-positive cells (arrow). (a) Gp null, Ad.null. (b) Gp eNOS, Ad.eNOS. (c) Gp iNOS, Ad.iNOS. (d) Gp e+i, Ad.eNOS plus Ad.iNOS. Strong expression of MMP-1 was observed in the lesions of Gps null, iNOS, and e+i. The expression was decreased in Gp eNOS. Original magnification, × 100. Lower: expression of TUNEL-positive apoptotic cells (arrow). (e) Gp null. (f) Gp eNOS. (g) Gp iNOS. (h) Gp e+i. Apoptotic cells were detected in Gps null, iNOS and e+i. However, apoptotic cells were rare in Gp eNOS. The scale bar represents 50 μm.

3.7. Nitrite and nitrate (NO_2^-/NO_3^-) and detection of aortic superoxide generation

Levels of NOx in medium (sum of NO_2^- and NO_3^-) in each group are shown in Table 1. iNOS treatment increased NOx in the regular control group of rabbits, but not in atherosclerotic rabbits (data not shown). The chemiluminescence signals from O_2^- production were greater in the aortae of iNOS gene-transfected groups, and the eNOS gene-transfected groups showed a slight decrease (Table 1). As an additional experiment described in Section 2.2, we separately prepared rabbits fed with a regular diet, and gene transfer of eNOS or iNOS was performed using dispatch catheter. NOx was increased, and O_2^- was not increased in the aortae from eNOS gene transfer rabbit as well as those from iNOS gene transfer rabbits (data not shown).

3.8. Immunocytochemical analysis

Atheroma in the abdominal aorta was composed of many macrophage-derived foam cells and intimal smooth muscle cells (Fig. 5). Gene transfer of Ad.eNOS not only reduced the area of atherosclerosis, but also decreased the area stained by the macrophage antibody and the areas positive for $ONOO^-$ established by nitrotyrosine staining (Fig. 5). The area stained by the smooth muscle cell actin was not different among the six groups, although it tended to be higher in the eNOS groups. MMP-1 (interstitial collagenase), a matrix metalloproteinase that initiates collagen degradation, was localized predominantly in macrophages. Although the difference did not reach the level of statistical significance, the expression of MMP-1 tended to be decreased in vessels of Gp eNOS and Gp heNOS (Fig. 6). A TUNEL-positive area was observed around a necrotic core in the atheroma as an apoptosis-susceptible area. The apoptosis-susceptible area seemed to be decreased in Gp eNOS and Gp heNOS; however, these differences were not statistically significant (Fig. 6).

4. Discussion

In the present study, in vivo gene transfer of eNOS, but not that of iNOS, resulted in a regression of advanced atherosclerosis and an improvement of EDR. This study has four major findings. First, NOS expression was increased throughout the vessels after transfection, demonstrating the highly efficient adenovirus-mediated gene transfer into severely atherosclerotic arteries. Second, adenovirus-mediated transfer of the eNOS gene alone restored EDR in atherosclerotic vessels. Third, eNOS gene transfer regressed atherosclerosis, and this effect appeared to have been due to a decrease of tissue lipids, although apoptosis or a decrease of extracellular matrix components may also have played a role. Finally, transfection with the iNOS gene failed to improve EDR and did not regress atherosclerosis. Further, simultaneous transfection of both the eNOS and iNOS genes also failed to improve EDR and did not regress atherosclerosis. In other words, transfection of iNOS blocked the beneficial effect of eNOS transfection.

4.1. Highly efficient adenovirus-mediated gene transfer in severe atherosclerosis

Gene transfers of NOS isoforms have been reported previously [9–12,23–27]. However, there have been only a few reports of in vivo gene transfer in advanced atherosclerotic vessels [9]. These studies used a high-cholesterol diet to induce atherosclerosis, resulting in patchy lesions that complicated the evaluation of gene transfer. In this study, we induced severe atherosclerosis by balloon injury and a high-cholesterol diet, resulting in severe atherosclerosis around the whole luminal area of vessels. The successful expression of the transgene (eNOS or iNOS) was confirmed by immunohistochemistry and Western blotting. We employed a 3-min perfusion at 6 atm. This choice was based on a previous study in which the efficacy of gene transfer was enhanced at a pressure greater than 4 atm, and in which no change in efficacy occurred between 2 and 40 min of perfusion [24]. Thahlil et al. [25] reported that the transduction rate is lower in medial smooth muscle cells than in the neointima or endothelium. Our data are almost identical to theirs. We used the same volumes of Ad.eNOS and Ad.iNOS, and separately used a 10-times higher titer of Ad.eNOS to evaluate whether or not the anti-atherosclerotic effect was dependent on the amount of NO.

4.2. Restoration of NO function of advanced atherosclerosis by Ad.eNOS

Gene transfer of eNOS remarkably improved the severely impaired EDR in atherosclerosis. The amount of transgene used in our experiment cannot be directly compared to that in the report by Ooboshi et al. [9]; however, the improvement of EDR by in vivo eNOS gene transfer in the present study is comparable with their report. In the present study, the animals receiving a high eNOS transfection (Gp heNOS) did not show any remarkable change in EDR or in the area of atherosclerosis compared to those receiving a smaller amount of the transgene (Gp eNOS). This finding suggest that the efficiency of the transgene might not be dose-dependent, and that a high dose of gene transfer may be insufficient to achieve a restoration of impaired EDR and complete regression. Regarding the mechanism of EDR improvement, we first hypothesized that regression of atherosclerosis could improve EDR, as the severity of atherosclerosis is inversely correlated with the impairment of EDR [15]. However, in the present study, the EDR improvement was much larger than that of the atherosclerosis regression. We speculated that EDR improvement occurs when NO bioavailability improves as a result of eNOS gene transfer, in turn related to the regression of

atherosclerosis. In fact, basal NO (as evaluated by tone-related basal NO release, NOx from vessels, and tissue cGMP concentration) was increased by eNOS gene transfer, but not by iNOS gene transfer. In the present study, the decrease level of O_2^- due to eNOS gene transfer also increased NO bioavailability.

4.3. The mechanisms of regression of atherosclerosis in response to eNOS

The pathological findings in the abdominal aortae of the present study were similar to previous findings in coronary arteries; i.e., in both cases the vessels were rich in macrophage-derived foam cells and lipids [15]. In the present study, eNOS gene transfer facilitated a significant regression of lesions, as well as a decrease in macrophages, indicating that the atheroma was stabilized. We previously established that there is a significant inverse relation between basal NO and the severity of atherosclerosis [13,15], and our present data suggest that this relation is involved in the NO release after eNOS gene transfer. Although previous studies have investigated the possibility of the regression of atherosclerosis by in vivo gene transfer [9,26–28], this might be the first demonstration of regression in a model of severe atherosclerosis induced by balloon injury and a high-cholesterol diet. The regression may be caused by the absorption of tissue lipid, while a cell decrease due to apoptosis or a decrease of the extracellular matrix such as collagen fibers may be a concern (Table 1 and Fig. 6). Absorption of tissue lipid can be caused by NO released from transferred eNOS, and we can speculate that HDL may be partially related to this absorption through increased NO release [29]. The apoptosis-suspected area by Tunnel staining tended to be small in Gp eNOS and Gp heNOS. Because $ONOO^-$ has cytotoxicity and the decreased level of O_2^- by eNOS gene transfer may contribute to a reduction in the substrate of $ONOO^-$, it could contribute to apoptosis. We cannot fully rule out the possibility that cell death occurred before our observation, because the effect of adenovirus gene transfer has been reported to peak at 3 days after transfection [27]. The role of apoptosis in regression should be elucidated further. Quian et al. [28] reported that monocyte recruitment occurred fairly quickly—i.e., within 24 h—after Ad.nNOS gene transfer. We speculate that a similar mechanism might occur by Ad.eNOS treatment for advanced atherosclerosis. We cannot fully rule out the possibility that other mechanism is responsible for regression, since our examination was made 7 days, rather than 24 h, after gene transfer. The tendency of a decrease in the MMP1-positive area supports the hypothesis that eNOS gene transfer stabilized the atheroma. The ratio of SMCs in atheroma did not differ significantly among the different groups of rabbits, although it tended to be relatively high in the Ad.eNOS transferred groups. We speculated that this occurs due to more decrease in macrophages in eNOS gene transfer group. Preliminarily, we did immunohistochemistry using anti-proliferating cellul nuclear antigen (PCNA), and TUNEL positive area looks like larger than anti-PCNA positive area in atheroma of each group on 7 days after gene transfer. We speculate the decrement in monocyte adhesion and the lipid in atheroma may be one of the possible mechanisms of regression, although other mechanisms may play a role. Further studies will be needed to establish the mechanism by which eNOS gene transfer regresses atherosclerosis.

4.4. Failure to improve impaired EDR and regression of severe atherosclerosis in response to Ad.iNOS, or Ad.eNOS plus iNOS

Neither gene transfer of iNOS nor that of eNOS plus iNOS improved EDR (Fig. 3). Transfection of empty vector with or without Ad.eNOS or Ad.iNOS did not affect EDR or the area of atherosclerosis compared to that of Gp eNOS, Gp iNOS, or Gp cont, indicating that the iNOS transgene not only impairs the improvement of EDR but also impairs the regression effect of eNOS. These data are somewhat contrary that iNOS is effective for improving vascular function, such as in the spastic arteries of various animal models [11,26,30]. As for the cause of the discrepant effects between previous and present studies, we speculate that the difference of enzyme activity of transferred gene between eNOS and iNOS, and the presence of intrinsic iNOS and O_2^- releasing enzymes in advanced atherosclerosis are important, although iNOS was transferred into iNOS-poor areas in previous studies [11,26,30]. In fact, the release of O_2^- was not increased, and that of NO was increased after iNOS gene transfer into normal aorta (3.5). The NO release from the Ad.eNOS-transfected atherosclerotic vessel was different from the Ad.iNOS-transfected vessel (Table 1). Both genes have the component of L-arginine (as substrate) binding site and BH4 (as cofactor) binding site. Ca^{2+}/calmodulin binding site is located in eNOS gene; however, it is already incorporated in iNOS gene. It is speculated that intracellular Ca^{2+} concentrations, even with transferred status, regulate NO release from eNOS and that iNOS is characterized by a greater specific activity, producing much larger quantities of NO in a calcium- and agonist-independent fashion [31]. eNOS releases O_2^- under conditions of depleted substrates or cofactors [32]. Large amount of transferred eNOS gene (Gp heNOS) may not be able to release NO by relative depletion of L-arginine or BH4. Intrinsic iNOS in atheroma is distributed in deep areas of atherosclerotic plaque (Fig. 2). These areas tend to be hypoxic with a relatively limited supply of arginine from the vasa vasorum or lumen [33,34]. The transferred iNOS was also distributed in all other components of blood vessels as well as in deep areas of the atherosclerosis. We suggest that iNOS releases O_2^- as well as NO, since iNOS is known to release O_2^- under conditions that deplete substrates, such as hypoxia, or that deplete arginine [35]. The report by Gunnett [12] may support our data. Macrophages or other inflammatory cells release O_2^- from NADPH oxidase or xanthine/xanthine

oxidase when stimulated by cytokines such as interferon γ, which also induce iNOS and co-localize in atheroma (data not shown). Nitrotyrosine, a marker of $ONOO^-$, was observed in the atherosclerotic regions, and its density was much greater in vessels transfected with iNOS and eNOS plus iNOS (Fig. 5). The response of O_2^- to a large amount of NO from transferred iNOS may have caused greater quantities of $ONOO^-$ and blocked the beneficial effect of NO from transferred eNOS. These differential effects between transgenes are interesting and important in gene therapy. As there are many O_2^- releasing enzymes such as NADPH oxidase and xanthine/xanthine oxidase as well as eNOS or iNOS, further studies like the experiment of iNOS gene transfer with or without antioxidant supplementation is necessary to elucidate the mechanisms.

4.5. Clinical significance of the present study

These findings may be relevant for improving blood flow and preventing thrombosis in advanced atherosclerotic arteries. The results of this study indicate that eNOS gene transfer should be clinically applied not only for prevention of atherogenesis, but also for the regression of advanced atherosclerosis. Because human atherosclerotic lesions, including intimal thickening, begin as early as childhood and by middle age are often quite prominent in the aorta and coronary arteries, hence regression is an important treatment tool. Regression and stabilization of atheroma is the main objective in the management of atherosclerotic lesions in humans. In the future, we expect that such clinical regression will be applicable for unstable angina or acute coronary syndrome. Although we must continue to work for a means of complete regression, the present results showed that eNOS gene transfer clearly improved the endothelial function and induced a regression of advanced atherosclerosis.

Acknowledgements

This study was supported by Japan Society for the Promotion of Science Award for Eminent Scientist, and Grant in aid for scientific research by Japanese Ministry of Education, Culture, Sports, Science and Technology, No. 09470166 and 13670704. We thank Wakako Adachi for her technical assistance.

References

[1] Lefer AM, Ma XL. Decreased basal nitric oxide release in hypercholesterolemia increases neutrophil adherence to rabbit coronary artery endothelium. Arterioscler Thromb 1993;13:771–6.
[2] Cooke JP. Role of nitric oxide in progression and regression of atherosclerosis. West J Med 1996;164:419–24.
[3] Cayatte AJ, Palacino JJ, Horten K, Cohen RA. Chronic inhibition of nitric oxide production accelerates neointima formation and impairs endothelial function in hypercholesterolemic rabbits. Arterioscler Thromb 1994;14:746–52.
[4] Ignarro LJ. Biological actions and properties of endothelium-derived nitric oxide formed and released from artery and vein. Circ Res 1989;65:1–21.
[5] Harrison DG, Armstrong ML, Freiman PC, Heistad DD. Restoration of endothelium-dependent relaxation by dietary treatment of atherosclerosis. J Clin Invest 1987;80:1808–11.
[6] Hayashi T, Esaki T, Muto E, Kano H, Iguchi A. Endothelium-dependent relaxation of rabbit atherosclerotic aorta was not restored by control of hyperlipidemia—the possible role of peroxynitrite. Atherosclerosis 1999;147:349–67.
[7] Aikawa M, Voglic SJ, Libby P, et al. Dietary lipid lowering reduces tissue factor expression in rabbit atheroma. Circulation 1999;100: 1215–22.
[8] Nabel EG, Nabel GJ. Complex models for the study of gene function in cardiovascular-biology. Annu Rev Physiol 1994;56:741–61.
[9] Ooboshi H, Toyoda K, Faraci FM, Lang MG, Heistad DD. Improvement of relaxation in an atherosclerotic artery by gene transfer of endothelial nitric oxide synthase. Arterioscler Thromb Vasc Biol 1998;18:1752–8.
[10] Von der Leyen HE, Gibbons GH, Dzau VJ, et al. Gene therapy inhibiting neointimal vascular lesion-in vivo transfer of endothelial nitric oxide synthase gene. Proc Natl Acad Sci U S A 1995;92: 1137–41.
[11] Shears II LL, Kibbe MR, Murdock AD, et al. Efficient inhibition of intimal hyper-plasia by adenovirus-mediated inducible nitric oxide synthase gene transfer to rats and pigs in vivo. J Am Coll Surg 1998;187:295–306.
[12] Gunnett CA, Lund DD, Heistad DD, et al. NO-dependent vasorelaxation is impaired after gene transfer of inducible NO-synthase. Arterioscler Thromb Vasc Biol 2001;21:1281–7.
[13] Esaki T, Hayashi T, Muto E, Kuzuya M, Iguchi A. Expression of inducible nitric oxide synthase in T lymphocytes and macrophages of cholesterol-fed rabbits. Atherosclerosis 1997;128:39–47.
[14] Chen AF, O'Brien T, Katusic ZS. Transfer and expression of recombinant nitric oxide synthase genes in the cardiovascular system. Trends Pharmacol Sci 1998;19:276–86.
[15] Hayashi T, Kano H, Thakur NK, Sumi D, Iguchi A. Physiological concentration of 17 β estradiol retards the progression of severe atherosclerosis induced by cholesterol diet plus balloon injury via NO. Arterioscler Thromb Vasc Biol 2000;20:1613–21.
[16] Sumi D, Hayashi T, Jayachandran M, Iguchi A. Estrogen prevents destabilization of endothelial nitric oxide synthase mRNA induced by tumor necrosis factor α. Life Sci 2001;69:1651–60.
[17] Hayashi T, Ignarro LJ, Fukuto JM, Chaudhuri G. Basal release of nitric oxide from aortic rings is greater in female rabbits than in male rabbits. Proc Natl Acad Sci U S A 1992;89:11259–63.
[18] Lipid Research Clinics Program Manual of Laboratory Operations. vol. 1, ed. 2. US Dept. of Health, Education and Welfare, Publ. No. (NIH). Washington, DC, US. Govt. Printing Office, pp. 1–76, 1982.
[19] Gaskell SJ, Finlay EM, Pike AW. Analyses of steroids in saliva using highly selective mass spectrometric techniques. Biomed Mass Spectrom 1980;7:500–4.
[20] Hayashi T, Muto E, Iguchi A, et al. Dehydroepiandrosterone retards atherosclerosis formation through the conversion to estrogen—the possible role of nitric oxide. Arterioscler Thromb Vasc Biol 2000; 20:782–92.
[21] Weiner BH, Ockene IS, Hoogasian JJ. Inhibition of atherosclerosis by cod-liver oil in a hyperlipidemic swine model. N Engl J Med 1986;315:841–5.
[22] Esaki T, Hayashi T, Muto E, Kano H, Thakur NK, Iguchi A. Expression of inducible nitric oxide synthase correlates with the incidence of apoptotic cell death in atheromatous plaques of human coronary arteries. Nitric Oxide: Biol Chem 2000;4:561–71.
[23] Lund DD, Faraci FM , Miller FJ Jr., Heistad DD. Gene transfer of endothelial nitric oxide synthase improves relaxation of carotid arteries from diabetic rabbits. Circulation 2000;101:1027–33.
[24] Chapman GD, Lim CS, Gammon RS, et al. Gene transfer into coro-

nary arteries of intact animals with a percutaneous balloon catheter. Circ Res 1992;71:27–33.
[25] Thahlil O, Brami M, Feldman LJ, Branelec D, Steg PG. The dispatch catheter as a delivery tool for arterial gene transfer. Cardiovasc Res 1997;33:181–7.
[26] Kibbe MR, Tzeng E, Gleixner SL, et al. Adenovirus-mediated gene transfer of human inducible nitric oxide synthase in porcine vein grafts inhibits intimal hyperplasia. J Vasc Surg 2001;34:156–65.
[27] Channon KM, Qian H, Neplioueva V, et al. In vivo gene transfer of nitric oxide synthase enhances vasomotor function in carotid arteries from normal and cholesterol-fed rabbits. Circulation 1998;98: 1905–11.
[28] Qian H, Neplioueva V, Shetty GA, Channon KM, George SE. Nitric oxide synthase gene therapy rapidly reduces adhesion molecule expression and inflammatory cell infiltration in carotid arteries of cholesterol-fed rabbits. Circulation 1999;99:2979–82.
[29] Tretjakovs P, Kalnins U, Dabina I, et al. Plasma HDL-cholesterol has an effect on nitric oxide production in coronary heart disease patients without LDL hypercholesterolemia. Med Sci Monit 2000;6:507–11.
[30] Fukumoto Y, Shimokawa H, Takeshita A, et al. Vasculoprotective role of inducible nitric oxide synthase at inflammatory coronary lesions induced by chronic treatment with interleukin-1 beta in pigs in vivo. Circulation 1997;96:3104–11.
[31] Morris SM Jr., Billiar TR. New insights into the regulation of inducible nitric oxide synthases. Am J Physiol 1994;266:E829–39.
[32] Vasquez-Vivar J, Martasek P, Whitsett J, Joseph J, Kalyanaraman B. The ratio between tetrahydrobiopterin and oxidized tetrahydrobiopterin analogues controls superoxide release from endothelial nitric oxide synthase: an EPR spin trapping study. Biochem J 2002;362:733–9.
[33] Kai H, Kuwahara F, Imaizumi T, et al. Coexistence of hypercholesterolemia and hypertension impairs adventitial vascularization. Hypertension 2002;39:455–9.
[34] Barker SG, Tilling LC, Martin JF, et al. The adventitia and atherogenesis: removal initiates intimal proliferation in the rabbit which regresses on generation of a neoadventitia. Atherosclerosis 1994;105: 131–44.
[35] Xia Y, Zweuer JL. Superoxide and peroxynitrite generation from inducible nitric oxide synthase in macrophages. Proc Natl Acad Sci U S A 1997;94:6954–8.

ORIGINAL ARTICLE

doi: 10.1111/j.1463-1326.2004.00393.x

NADPH oxidase inhibitor, apocynin, restores the impaired endothelial-dependent and -independent responses and scavenges superoxide anion in rats with type 2 diabetes complicated by NO dysfunction

T. Hayashi, P. A. R. Juliet, H. Kano-Hayashi, T. Tsunekawa, D. Dingqunfang, D. Sumi, H. Matsui-Hirai, A. Fukatsu and A. Iguchi

Department of Geriatrics, Nagoya University Graduate School of Medicine, Nagoya, Japan

Objective: We investigated the effect of apocynin, an NADPH oxidase inhibitor, in the impairment of vascular responses in Otsuka Long-Evans Tokushima Fatty (OLETF) rats (type 2 diabetic rat model) with or without (w/wo) *N*-nitro-L-arginine methyl ester treatment.

Methods: Male OLETF and littermate Long-Evans Tokushima Otsuka (LETO) (28 weeks old) rats were separated as follows: LETO w/wo apocynin (Gp C, Gp C-apo), OLETF w/wo apocynin (Gp DM, Gp DM-apo) and OLETF plus L-nitro arginine acetate ester w/wo apocynin (Gp DMLN, Gp DMLN-apo). Five days after, peritoneal macrophages were stimulated with thioglycolate. Two days after, they were evaluated.

Results: Plasma glucose and lipid levels remained unchanged. Acetylcholine-induced nitric oxide-dependent (NO-dependent) relaxation and nitroglycerin-induced NO-independent relaxation were improved in the Gp DMLN-apo, compared with that in Gp DMLN. Tone-related basal NO release and plasma NO_2^- and NO_3^- tended to be lower in Gp DM and Gp DMLN groups. The increased amount of superoxide anion released from macrophages in Gp DM and Gp DMLN was restored by apocynin. Intimal thickening was observed in aortae of Gp DM and Gp DMLN animals; however, there was little in aortae of Gp DM-apo and Gp DMLN$^-$ apo rats. Increased tumour necrosis factor-α (TNF-α) in the Gp DM and Gp DMLN was also restored by apocynin treatment.

Conclusion: Apocynin restores the impairment of endothelial and non-endothelial function in diabetic angiopathy in OLETF without changing plasma glucose and lipid levels. NO and O_2^- may play a role in this process by decreasing TNF-α levels.

Keywords: NADPH oxidase, nitric oxide, diabetes mellitus, superoxide

Received 13 March 2004; returned for revision 18 April 2004; revised version accepted 19 April 2004

Introduction

The atherogenic process is characterized by an early deficit in nitric oxide (NO) [1,2]. Chronic inhibition of NO, in addition to a high-cholesterol diet, induces severe atherosclerosis [3]. Coronary risk factors such as hyperlipidaemia and diabetes are known to impair NO function, and its impairment becomes severe as the number of risk factors suffered is increasing [3,4]. In diabetes, large-artery

Correspondence:
T. Hayashi, Department of Geriatrics, Nagoya University Graduate School of Medicine, Tsuruma-cho, Showa-ku, Nagoya 466-8550, Japan.
E-mail:
hayashi@med.nagoya-u.ac.jp

ischaemic disease is a major problem, especially in the elderly, and complications associated with other coronary risk factors are known to facilitate ischaemia as well as the growth of lesions [5]. The restoration of impaired endothelial function, represented by impaired endothelium-dependent relaxation (EDR) in the diabetic vessel, is important for the stabilization of atheroma. However, restoration of EDR in patients with diabetes has not been consistently observed [6,7]. Clinical and experimental evidence has not yet demonstrated the sufficient stabilization of diabetic vascular complications.

Superoxide production by vascular tissues and its interaction with NO plays an important role in diabetic and atherosclerotic vascular pathophysiology [8,9]. Abnormal vascular endothelial function and atherosclerosis are prominent features of diabetes mellitus, and evidence from experimental studies suggests that increased superoxide production accounts for a significant proportion of the NO deficit in diabetic vessels [10,11]. In addition to NO scavenging, superoxide may alter the activity and the regulation of endothelial NO synthase in endothelial cells, and superoxide may also have other potentially proatherogenic effects on smooth muscle cell proliferation, inflammatory cell recruitment and redox-sensitive gene expression [12].

Potential sources of vascular superoxide production include NAD(P)H-dependent oxidases, xanthine oxidase, lipoxygenase, mitochondrial oxidases and NO synthases. NAD(P)H oxidases appear to be the principal source of superoxide production in several animal models of vascular disease, including diabetes [9]. Furthermore, NAD(P)H oxidase subunits and activity has been observed in human blood vessels, including atherosclerotic coronary arteries, suggesting that this oxidase system plays an important role in a number of vascular disease states [12]. Despite the importance of increased superoxide production in endothelial dysfunction and vascular disease in diabetes, the characteristics and mechanisms of vascular superoxide production in diabetes remain only partially defined [13–15]. Accordingly, we evaluated the sources and relative magnitude of superoxide production in arteries taken from type 2 diabetic rats with or without (w/wo) *N*-nitro-L-arginine methyl ester (L-NAME) treatment, which can severely damage endothelial function; these rats were thought to be a suitable because the model status are similar to that of diabetes complicated by other coronary risk factors. In particular, we sought to investigate the NAD(P)H oxidase system by using a NADPH oxidase inhibitor, apocynin, and we also examined the putative role of endothelial NO synthase (eNOS) dysfunction in contributing to vascular superoxide production. The underlying mechanism leading to the increase of superoxide produced by NADPH oxidase, eNOS, etc., is thought to involve TNF-α, which regulates NADPH oxidase and inducible NOS (iNOS) at the promotor level. Furthermore, we previously reported that TNF-α, which is known to be present in high levels in patients with atherosclerosis, destabilizes eNOS, and the destabilization was prevented by treatment with estradiol [16]. In addition, TNF-α levels are known to be increased in patients with poor blood glucose control and with insulin resistance, and thus TNF-α is thought to play a role in diabetic angiopathy [16]. This line of reasoning led us to measure the plasma levels of TNF-α in the rat models used in the present study.

Materials and Methods

Chemicals

Acetylcholine chloride (ACh), prostaglandin F2α (PGF2α), indomethacin and L-NAME (NO synthase inhibitor) were purchased from Sigma Chemical Co. (St Louis, MO, USA). Nitroglycerin was obtained from Nihon Kayaku Co. Ltd. (Tokyo, Japan). Determination of TNF-α was carried out by enzyme-linked immunosorbent assay (ELISA) kit [16].

Animals

Male Otsuka Long-Evans Tokushima Fatty (OLETF) rats (type II diabetic rats, 28 weeks old) and littermate Long-Evans Tokushima Otsuka (LETO) rats (28 weeks old) were obtained from the Otsuka Pharmaceutical Company (Tokushima City, Japan) [13], and they were divided into six groups as follows: Gp C, LETO was fed regular chow; Gp C-apo, LETO was fed regular chow with apocynin (NADPH oxidase inhibitor, 30 mg/kg/day); Gp DM, OLETF was fed regular chow; Gp DM-apo, OLETF was fed regular chow with apocynin; Gp DMLN, OLETF was fed regular chow with L-NAME (100 mg/kg/day) and Gp DMLN-apo was fed regular chow with apocynin plus L-NAME. The rats were housed with free access to water. Five days after treatment of each condition as described above, their peritoneal macrophages were stimulated with the peritoneal injection of thioglycolate [17]. Two days after the injection, they were exsanguinated and evaluated. All experiments were conducted in accordance with institutional guidelines for animal research.

Blood Sampling

The following measurements were also carried out before and after the treatment: body weight, fasting plasma glucose and insulin concentrations, serum total

cholesterol, triglycerides and high-density lipoprotein (HDL) cholesterol. The following factor, which might be involved in the mechanism, was also investigated: TNF-α. ELISA kits were used for the measurements (JIMRO, Takasaki, Japan).

Vascular Response

Seven days after treatment, the rats (each group n = 6) were sacrificed by exsanguination after being anaesthetized with pentobarbital (50 mg/kg IP). Vascular responses were investigated as described previously [18]. Briefly, aortae were cut into 2-mm wide transverse rings. Those were stretched to their optimal force, which was predetermined at the contraction to 122 mM KCl, and were mounted in chambers filled with Krebs' Henseleit solution at 37 °C. The response of aortic rings to ACh and normal triglyceride were determined under submaximal contraction by PGF2α (2.6×10^{-6} M). Tone-related basal NO release, contractile responses to L-monomethyl-arginine (L-NMA) was assessed under moderate tone (about 40% contraction by KCl) induced by PGF2α (0.8×10^{-6} M) [18]. In some studies, indomethacin (5×10^{-6} M) was added in to the chambers to rule out the contribution of prostanoids.

Measurement of Nitrite and Nitrate (NO_2^-/NO_3^-) and Detection of Aortic Superoxide Generation

Plasma NOx (sum of nitrite and nitrate, NO_2^-/NO_3^-) was measured using NO detector-HPLC system (ENO10; Eicom Co., Kyoto, Japan), which was used as previously reported [19].

Detection of Aortic Superoxide Anion (O_2^-) Generation from Aorta and Intracellular Redox State of Peritoneal Macrophages

Formation of O_2^- from the vessel was assayed by measuring the intensity of chemiluminescence probes in the presence of one of the Cypridina luciferin analogs, 2-methyl-6-(p-methoxyphenyl)-3,7-dihydroimidazo-1,2-a pyrazine-3-one (MCLA) [20]. In brief, the O_2^- generation signal from the 2 mm length of vessel was detected by a luminescence reader (BLR-201, Aloka Co., Tokyo, Japan). To ensure the specificity of MCLA to detect O_2^-, increasing concentrations of superoxide dismutase (1–50 U/ml) were added to the tissues. Intracellular redox state levels of peritoneal macrophages stimulated by thioglycolate for 2 days were measured with a fluorescent dye, CDCFH diacetate bis-AM ester, a non-polar compound that is converted into a non-fluorescent polar derivative (CDCFH) by cellular esterases after incorporation into cells. CDCFH is membrane-impermeable and rapidly oxidized to the highly fluorescent carboxydichlorfluorescein in the presence of intracellular hydrogen peroxide and peroxidases. The fluorescence intensity of each point was measured by flow cytometry and calculated with untreated control cells as a standard [21]. The excitation wavelength was 510–530 nm. Relative fluorescence intensities were measured.

Histological Evaluation of Atherosclerosis

Cross-sections of the aorta adjacent to segments for vascular responses were examined [22]. Briefly, the contours of the lumen and the internal elastic lamina (IEL) were traced. The mean surface involvement by atherosclerotic lesion (intimal thickening) per vessel (extent) was calculated after dividing the lesion circumference by the circumference of the IEL. The circumferences of the lesion and the healthy region were defined as the circumferences of the respective parts of the IEL. The area occupied by atherosclerotic lesions (total lesion burden: size/thickness) was defined as the percentage area bounded by the lumen and the IEL for luminal area.

Immunohistochemical Study

Tissues were sectioned to 5-μm slices [8]. Primary monoclonal antibodies (anti-macrophages, anti-smooth muscle cells, anti-endothelial NO synthase, anti-inducible NO synthase or anti-nitrotyrosine) were applied. Sections were incubated with biotinylated immunoglobulins and incubated with horseradish peroxidase-labelled avidin solution (Vecstatin Elite, Vector Laboratories, Burlingame, CA, USA). Negative controls included the substitution of primary antibody with irrelevant antibodies. There were no cross-reactions between anti-eNOS and anti-iNOS antibodies. Each field was scored for number of each antibody positive cells on the slides and analysed statistically as described by previous report [23]. Five samples were prepared from each rat.

Statistics

Data are presented as mean ± s.e.m. The student's *t*-test was used and Kruskal–Wallis one-way ANOVA was used for multiple comparisons. $p < 0.05$ is considered as significant. Statistical calculations were performed using STAT VIEW software (version 5.01-SAS Institute, Cary, NC, USA).

Results

Body Weight and Blood Sampling

The plasma biochemical profiles are shown in table 1. There were no significant differences among the six groups before or after treatment with regard to the body weight, serum total protein, fasting plasma glucose, total and HDL cholesterol and triglycerides. The plasma concentrations of TNF-α had significantly increased in the Gp DM and Gp DMLN groups, whereas no change was observed in the following groups: Gp C, C-apo, DM-apo and DMLN-apo (table 1). After treatment, the plasma concentration of NOx (sum of nitrite and nitrate) did not change significantly in Gp DM compared with Gp C, however, it was decreased significantly in Gp DMLN and Gp DMLN-apo.

Vascular Response

Basal NO release was decreased in Gp DM and Gp DMLN, but such a decrease was not observed in the following groups: Gp C w/wo apocynin, Gp DM-apo or Gp DMLN-apo (figure 1). Acetylcholine-induced NO-dependent relaxation was impaired in the Gp DM group and was particularly impaired in the Gp DMLN. However, this type of relaxation improved in the Gp DM-apo and Gp DMLN-apo, as compared to that in the corresponding groups without apocynin treatment (Gp DM and DMLN) (figure 1). Nitroglycerin-induced endothelium-independent relaxation was also slightly impaired in the Gp DM and DMLN groups, but no change was observed in the other groups.

Detection of Aortic Superoxide Anion Generation and Intracellular Radicals State of Peritoneal Macrophages

The chemiluminescence signals as superoxide anion production from aorta remarkably increased in Gp DM-LN and slightly increased in Gp DM as compared with LETO groups. O_2^- from aorta in Gp C was 0.35 ± 0.18 Kcpm/mg protein. Superoxide anion production decreased in Gp DM-apo when compared with Gp DM-LN (figure 2 upper). The amounts of intracellular redox released from peritoneal macrophages were increased in the OLETF groups, especially in the DMLN group, as compared with the LETO groups (figure 2 lower). However, these levels were restored in the DM-apo and DMLN-apo groups. In particular, DMLN-apo restored the amount of superoxide anion to the normal level.

Histological Evaluation of Atherosclerosis

Atherosclerotic changes were observed in the aortae from Gp DMLN rats (11.3 ± 2.1, $4.8 \pm 1.7\%$ in surface involvement, area occupied by lesion); however, there were few such changes observed in the aortae from the Gp DM (5.3 ± 1.4, $2.1 \pm 0.8\%$), Gp DM-apo (2.3 ± 1.1, $1.1 \pm 0.4\%$) and Gp DMLN-apo rats (4.7 ± 1.3, $1.4 \pm 0.5\%$).

Immunohistochemical Study

Monocytes/macrophages were attached to the endothelium and were distributed only to a small extent in the sub-intima of the Gp DM group rats; these cells were present in modest amounts in the sub-intima of the Gp DMLN animals, but not observed in the other groups (figure 3 upper). A few smooth muscle cells were observed in the sub-intima in the Gp-DM, Gp-DMLN, Gp DM-apo and Gp DMLN-apo groups, but not in the other two groups (data not shown). iNOS was slightly apparent in the sub-intima of the Gp DM and Gp DMLN, but absent in the other groups (figure 3 lower panel). Peroxynitrite, as visualized by staining with nitrotyrosine, was rarely present, but it was observed in small concentration in the sub-intima of the Gp DM and

Table 1 Biochemical and NO related profile

	B.W. (g)	T.P. (g/dl)	FBS (mg/dl)	T.Chol (mg/dl)	T.G. (mg/dl)	HDL-C (mg/dl)	NO_2^-/NO_3^- (μM)	TNF-α (pg/ml)
Gp C	633.0 + 24.3	8.1 + 1.2	83.0 + 21.3	75.2 + 9.8	31.8 + 4.2	30.4 + 7.2	36.4 + 3.5	13.1 + 3.6
Gp Capo	612.6 + 27.3	7.8 + 1.2	80.6 + 17.3	59.5 + 10.6	29.8 + 4.0	29.3 + 6.2	40.5 + 3.6	10.3 + 2.4
Gp DM	690.5 + 70.4	6.9 + 2.5	263.1* + 35.0	87.8 + 14.1	34.9 + 4.1	29.5 + 7.7	33.2 + 4.1	25.5 + 4.5
Gp DM-apo	64.7 + 83.3	7.2 + 1.9	250.5 + 52.7	69.3 + 23.8	30.9 + 5.1	30.3 + 4.5	36.9 + 4.6	13.8* + 2.5
Gp DMLN	625.0 + 10.7	6.9 + 1.7	252.0 *+ 37.6	66.7 + 15.7	34.7 + 8.5	35.3 + 7.7	22.5* + 4.5	32.8* + 4.6
Gp DMLN-apo	612.5 + 101.4	6.9 + 1.8	251.1 + 47.2	74.9 + 19.1	35.3 + 4.2	38.1 + 7.1	25.8* + 4.2	16.7# + 2.6

B.W., body weight; FBS, fasting blood sugar; HDL-C, High-density lipoprotein cholesterol; T.Chol, Total Cholesterol; T.G., Triglyceride; T.P., Total Protein; TNF-α, tumour necrosis factor-α. *$p < 0.05$ vs. Gp C, #$p < 0.05$ vs. Gp DMLN.

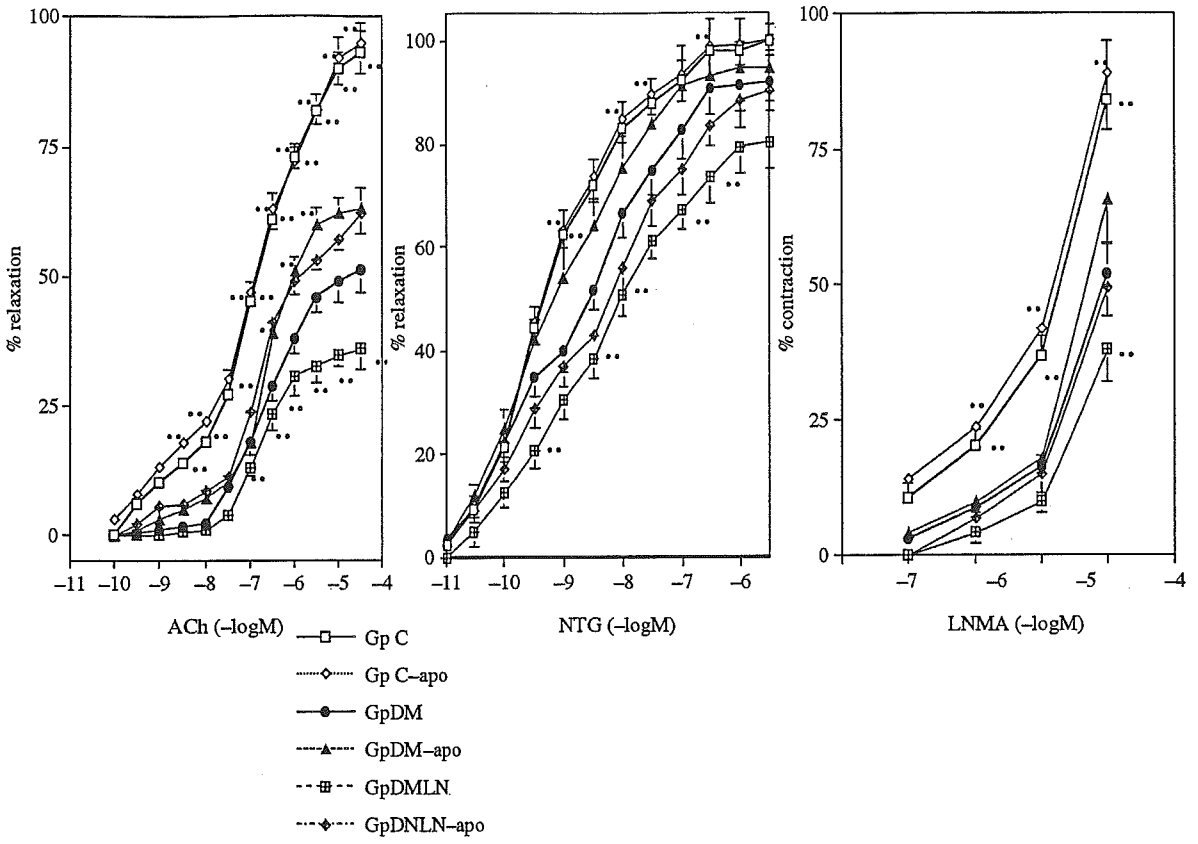

Fig. 1 Cumulative concentration response curves for each of the agonists in the abdominal aortae of six groups, which were precontracted by prostaglandin F2α: Gp C, Long-Evans Tokushima Otsuka (LETO) fed regular chow; Gp C-apo, LETO-fed regular chow with apocynin; Gp DM, Otsuka Long-Evans Tokushima Fatty (OLETF) fed regular chow; Gp DM-apo, OLETF-fed regular chow with apocynin; Gp DMLN, OLETF-fed regular chow with *N*-nitro-L-arginine methyl ester (L-NAME); Gp DMLN-apo fed regular chow with apocynin plus L-NAME. Left: Cumulative concentration-response curves for acetylcholine. Middle: Cumulative concentration-response curves for nitroglycerin. Right: Cumulative concentration-response curves for L-NMA; NOS inhibitor. % means the percentage vs. the magnitude of the contraction level by PGF2α. *$p < 0.05$, **$p < 0.01$ vs. Gp C.

DM-LN groups, but was not observed in the sub-intima of the other four groups. The staining area was almost same as that observed by iNOS antibody (data not shown).

Discussion

Abnormal vascular endothelial function and intimal thickening (atheromatous change) are common among the patients with diabetes mellitus, and increased superoxide production appears to be account for a significant proportion of the observed NO deficit status associated with diabetes [8–11]. Although potential sources of vascular superoxide production include NADPH-dependent oxidases, xanthine oxidase, lipoxygenase, mitochondrial oxidases and endothelial and inducible NO synthases, NADPH oxidase appears to be the principal source in several animal models of diabetes [9,12,13]. For this reason, we investigated the effect of apocynin, an NADPH oxidase inhibitor, in a diabetes model w/wo severe endothelial dysfunction. In the present study, there was only a slight release of superoxide anion from macrophages in the LETO groups w/wo apocynin; this release was increased in OLETF rats, and especially in the L-NAME-treated OLETF rats. However, apocynin treatment (Gp DM + apo and GP DMLN + apo) restored the levels of superoxide anion to the control level observed in the LETO groups. Furthermore, morphological changes in response to diabetes plus NO dysfunction were not evident in the apocynin treatment groups.

Our findings suggest two important and potentially related mechanisms that underlie these functional deficits. First, increased superoxide production in atherosclerosis and other pro-atherosclerotic states likely reduces NO bioactivity by a direct scavenging mechanism. The

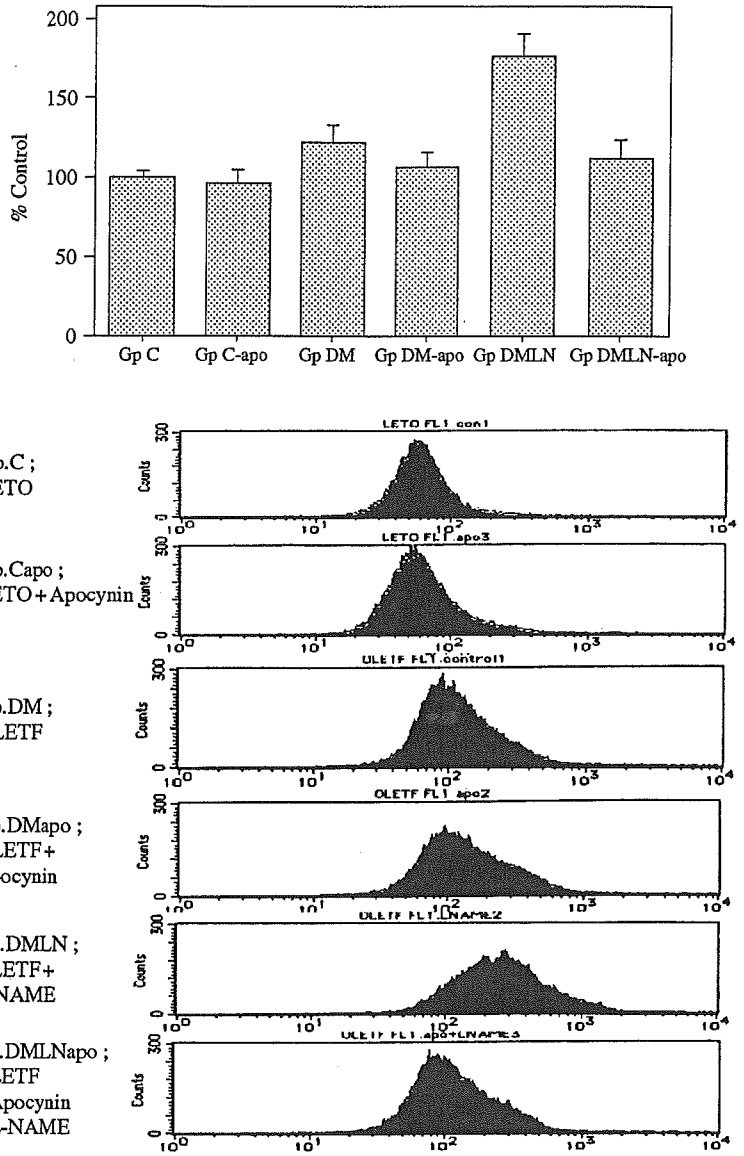

Fig. 2 Upper: Formation of O_2^- from vessel was assayed by MCLA methods. Gp C, Long-Evans Tokushima Otsuka (LETO) fed regular chow; Gp C-apo, LETO fed regular chow with apocynin; Gp DM, Otsuka Long-Evans Tokushima Fatty (OLETF) fed regular chow; Gp DM-apo, OLETF fed regular chow with apocynin; Gp DMLN, OLETF fed regular chow with *N*-nitro-L-arginine methyl ester (L-NAME); Gp DMLN-apo fed regular chow with apocynin plus L-NAME, $^*p < 0.05$ vs. of O_2^- from Gp C vessels. Lower: Superoxide anion release from peritoneal macrophages, which was evaluated by FACS Scan.

expression of NADPH oxidases have been shown in vascular cells and macrophages in atherosclerotic coronary arteries [11,12]. The effect of NADPH oxidase in this diabetes model was clearly demonstrated by the effectiveness of apocynin treatment, which basically reversed the impairment of endothelial function in the relevant groups in this study and decreased superoxide anion release from diabetic vessels and also decreased it from macrophages. The other mechanism underlying such functional deficits would be the uncoupling of NOS. Although eNOS in the vascular endothelium and iNOS in macrophages produce NO, they may be sources of superoxide production under certain conditions, due to the enzymatic uncoupling of L-arginine oxidation and oxygen reduction by the oxygenase and reductase domains of eNOS, respectively [24]. Recent studies have suggested that the reduced availability of the cofactor tetrahydrobiopterin (BH4) may result in eNOS or iNOS uncoupling, in turn responsible for the imbalance between NO production and superoxide production in diabetic vascular lesions [25]. It has been observed in diabetic vessels that hyperglycaemia increases NOS-dependent superoxide production in human endothelial cells and that mediates eNOS dysfunction in endothelial cells [26,27]. In studies of experimental diabetes in rats

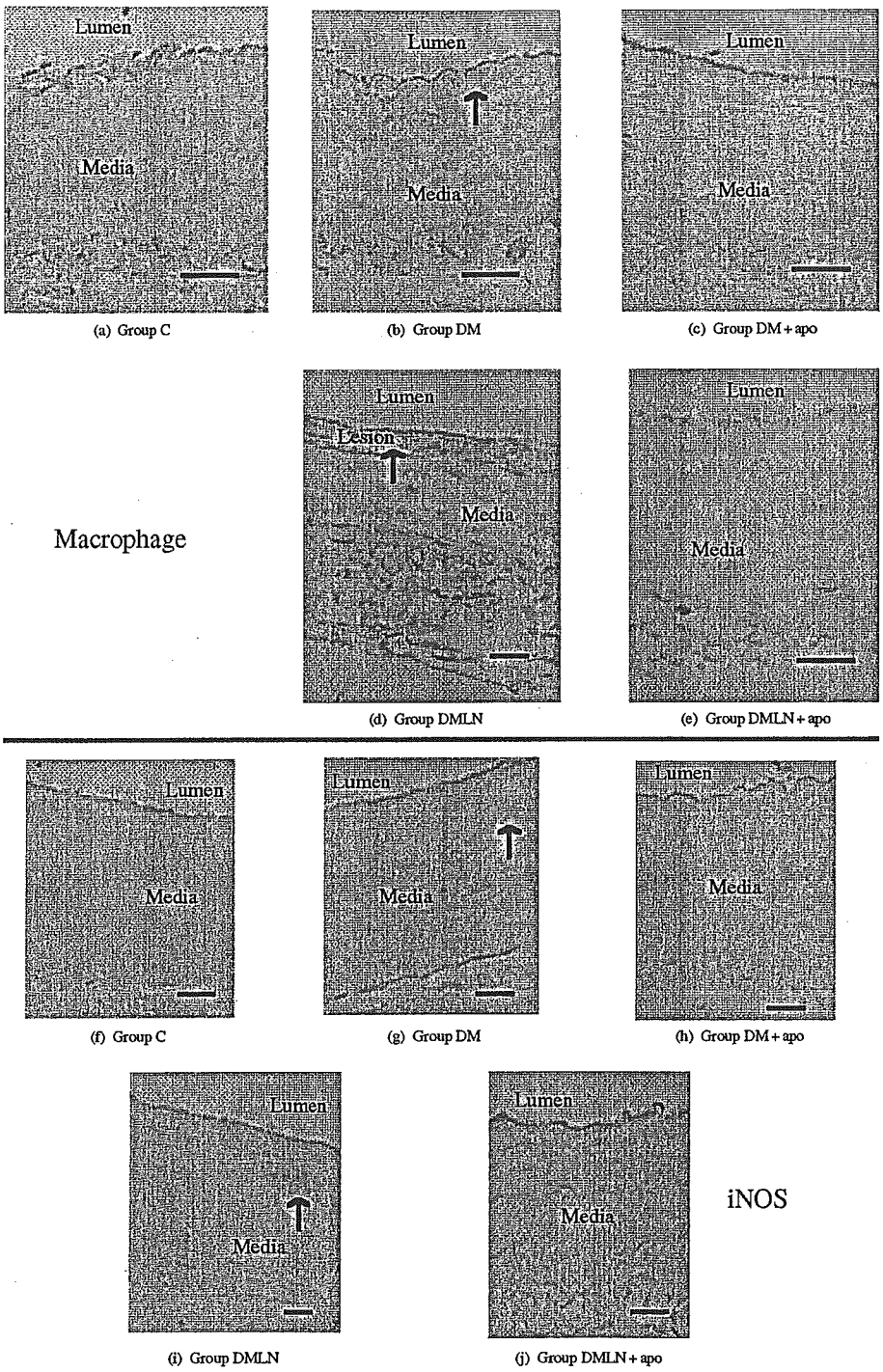

Fig. 3 The representative immunohistochemical staining of abdominal aortas. Upper: A section stained with a monoclonal antibody against macrophages (arrow) from (a) Gp C, Long-Evans Tokushima Otsuka (LETO); (b) Gp DM, Otsuka Long-Evans Tokushima Fatty (OLETF); (c) Gp DM-apo, OLETF with apocynin; (d) Gp DMLN, OLETF with *N*-nitro-L-arginine methyl ester (L-NAME); and (e) Gp DMLN-apo with apocynin plus L-NAME (original magnification ×150). Bar is 50 μM. Lower: A section stained with a monoclonal antibody against the marker of induced NO synthase (arrow) from (f) Gp C; (g) Gp DM; (h) Gp DM-apo; (i) Gp DMLN and (j) Gp DMLN-apo (original magnification ×100). Bar is 50 μM. Lumen: luminal area, Media: media, Lesion: atheromatous lesion.

and in atherosclerotic apolipoprotein E-knockout mice, in which both increased NAD(P)H oxidase activity and NOS dysfunction have been found to contribute to both increased total vascular superoxide production and reduced NO bioactivity [28]. Therefore, the up-regulation of vascular superoxide production by NAD(P)H oxidases may in turn lead to eNOS or iNOS uncoupling via the oxidation of BH4, which reduces NO production and further increases endothelial superoxide production.

In the present study, we studied the effect of L-NAME treatment on OLETF rats w/wo apocynin in order to investigate severe endothelial dysfunction in a diabetic animal model complicated by other coronary risk factors. Chronic NO inhibition by L-NAME treatment facilitates high-cholesterol-diet-induced atherosclerosis, and L-NAME treatment induces intimal thickening in rat models [3,29]. Landmark clinical trials such as the United Kingdom prospective diabetes study and 4S have demonstrated that strict control of complicated coronary risk factors such as hypertension and hypercholesterolemia are as important as the control of plasma glucose levels in the prevention of ischaemic cardiovascular events. One of the common mechanisms underlying these treatments is improving or restoring endothelial function such as NO bioavailability [30,31]. In our present study, it is interesting that apocynin successfully improved endothelial dysfunction and inhibited superoxide release from activated macrophages.

Apocynin (4′-hydroxy-3′-methoxy-acetophenone or acetovanilone), a non-toxic compound isolated from the medicinal plant *Picrohiza kuroa*, is a potent inhibitor of NADPH oxidase in stimulated human neutrophils (IC50 : 10 mM) [32]. An additional interesting aspect of apocynin is its very low toxicity (LD50 : 9 g/kg oral administration in mice) [33]. Apocynin inhibits neutrophil NADPH oxidase activity, thereby preventing the production of oxygen radicals [34–37]. Apocynin was reported to inhibit NADPH oxidase activity by the dissociation of p47 phox, which was the membranous component of NADPH oxidase from Gp 91 [36]. Our preliminary experiments using cultured macrophages and endothelial cells showed the same results (data not shown). This is the first report to investigate the usefulness of this NADPH oxidase inhibitor as a drug in a model of diabetic angiopathy. Our results suggest that the mechanism leading to this effect involves a decrease in the plasma TNF-α concentration. In the present study, blood glucose levels did not change in any of the groups. In this context, it should be noted that TNF-α has been shown to up-regulate NADPH oxidase in endothelial cells and diabetic vessels, and TNF-α was shown to inhibit the activation of eNOS, which in turn indirectly enhances eNOS uncoupling [38,39]. In liver, free radicals from NADPH oxidase in hepatic Kupffer cells play a predominant role in the pathogenesis of early alcohol-induced hepatitis by activating NF-kappa B, which activates the production of cytotoxic TNF-α [40]. Like this, superoxide anion from NADPH oxidase from endothelial cells and macrophages can activate NK-kappa B and then produce TNF-α.

In conclusion, we found that macrophages from diabetic rats produce high levels of superoxide. The level of superoxide was especially increased in diabetic rats with severe endothelial dysfunction resulting in NOS-inhibitor treatment. Apocynin, an NADPH oxidase inhibitor, reversed the endothelial dysfunction and prevented the atherosclerotic, morphological changes in diabetic rats regardless of whether or not they were subjected to NOS inhibition.

Acknowledgements

This study was supported in part by Grant-in-Aid no. 13670704 of the Japanese Ministry of Education and Japan Society for the Promotion of Science award for eminent scientist. We thank Wakako Adachi for her technical assistance.

References

1 Hayashi T, Kuzuya M, Funaki C, Kuzuya F. β-very low density lipoprotein inhibits endothelium dependent relaxation in atherosclerotic vessels. Blood Vessels 1989; **26:** 290–299.
2 Chester AH, O'Neil GS, Moncada S, Tadjkarimi S, Yacoub MH. Low basal and stimulated release of nitric oxide in atherosclerotic epicardial coronary arteries. Lancet 1990; **336:** 897–900.
3 Cayatte AJ, Palacino JJ, Horten K, Cohen RA. Chronic inhibition of nitric oxide production accelerates neointima formation and impairs endothelial function in hypercholesterolemic rabbits. Arterioscler Thromb 1994; **14:** 746–752.
4 Ignarro LJ. Biological actions and properties of endothelium-derived nitric oxide formed and released from artery and vein. Circ Res 1989; **65:** 1–21.
5 DeFronzo RA, Ferrannini E. Insulin resistance. A multifaceted syndrome responsible for NIDDM, obesity, hypertension, dyslipidemia, and atherosclerotic cardiovascular disease. Diabetes Care 1991; **14:** 173–194.
6 Harrison DG, Armstrong ML, Freiman PC, Heistad DD. Restoration of endothelium-dependent relaxation by dietary treatment of atherosclerosis. J Clin Invest 1987; **80:** 1808–1811.
7 Hayashi T, Esaki T, Muto E, Kano H, Iguchi A. Endothelium-dependent relaxation of rabbit atherosclerotic

aorta was not restored by control of hyper-lipidemia - the possible role of peroxynitrite. Atherosclerosis 1999; **147:** 349–367.

8 Sampson MJ, Gopaul N, Davies IR, Hughes DA, Carrier MJ. Plasma F2 isoprostanes. Direct evidence of increased free radical damage during acute hyperglycemia in type 2 diabetes. Diabetes Care 2002; **25:** 537–541.

9 Guzik TJ, West NE, Black E *et al.* Vascular superoxide production by NAD(P)H oxidase: association with endothelial dysfunction and clinical risk factors. Circ Res 2000; **86:** E85–E90.

10 Hink U, Li H, Mollnau H *et al.* Mechanisms underlying endothelial dysfunction in diabetes mellitus. Circ Res 2001; **88:** E14–E22.

11 Shinozaki K, Kashiwagi A, Nishio Y *et al.* Abnormal biopterin metabolism is a major cause of impaired endothelium-dependent relaxation through nitric oxide/O_2^- imbalance in insulin-resistant rat aorta. Diabetes 1999; **48:** 2437–2445.

12 Warnholtz A, Nickenig G, Schulz E *et al.* Increased NADH-oxidase-mediated superoxide production in the early stages of atherosclerosis: evidence for involvement of the renin-angiotensin system. Circulation 1999; **99:** 2027–2033.

13 Kagota S, Yamaguchi Y, Nakamura K, Kunitomo M. Altered endothelium dependent responsiveness in the aortas and renal arteries of Otsuka Long-Evans Tokushima Fatty (OLETF) rats, a model of non-insulin-dependent diabetes mellitus. General Pharmacol 2000; **34:** 201–209.

14 Haluzik M, Nedvidkova J, Skrha J. The influence of methylene blue and L-NAME on the development of streptozotocin-induced diabetes in rats. Sb Lek 1999; **100:** 213.

15 Rao VS, Santos FA, Silva RM, Teixiera MG. Effects of nitric oxide synthase inhibitors and melatonin on the hyperglycemic response to streptozotocin in rats. Vascul Pharmacol 2002; **38:** 127–130.

16 Tsunekawa T, Hayashi T, Suzuki Y *et al.* Plasma adiponectin plays an important role in improving insulin resistance with glimepiride in elderly type 2 diabetic subjects. Diabetes Care 2003; **26:** 285–289.

17 Thompson K, Maltby J, Fallowfield J, McAulay M, Millward-Sadler H, Sheron N. Interleukin-10 expression and function in experimental murine liver inflammation and fibrosis. Hepatology 1998; **28:** 1597–1606.

18 Hayashi T, Fukuto JM, Ignarro LJ, Chaudhuri G. Basal release of nitric oxide from aortic rings is greater in female rabbits than in male rabbits: implications for atherosclerosis. Proc Natl Acad Sci USA 1992; **89:** 11259–11264.

19 Hayashi T, Esaki T, Muto E *et al.* Dehydroepiandrosterone retards atherosclerosis formation through the conversion to estrogen-The possible role of nitric oxide. Arterioscler Thromb Vasc Biol 2000; **20:** 782–792.

20 Stevenson HC, Bonvini E, Favilla T *et al.* Characterization of purified cryopreserved human monocyte function in assays of superoxide production, accessory cell function, chemotaxis, and in fluorescent cell sorter analysis. J Leukoc Biol 1984; **36:** 521–531.

21 Skatchkov MP, Sperling D, Hink U, Anggard E, Munzel T. Quantification of superoxide radical formation in intact vascular tissue using a Cypridina luciferin analog as an alternative to lucigenin. Biochem Biophys Res Commun 1998; **248:** 382–386.

22 Weiner BH, Ockene IS, Hoogasian JJ. Inhibition of atherosclerosis by cod-liver oil in a hyperlipidemic swine model. N Engl J Med 1986; **315:** 841–847.

23 Esaki T, Hayashi T, Thakur NK *et al.* Expression of inducible nitric oxide synthase and Fas/Fas ligand correlates with the incidence of apoptotic cell death in atheromatous plaques of human coronary arteries. Nitric Oxide 2000; **4:** 561–571.

24 Vasquez-Vivar J, Kalyanaraman B, Martasek P *et al.* Superoxide generation by endothelial nitric oxide synthase: the influence of cofactors. Proc Natl Acad Sci USA 1998; **95:** 9220–9225.

25 Meininger CJ, Marinos RS, Hatakeyama K *et al.* Impaired nitric oxide production in coronary endothelial cells of the spontaneously diabetic BB rat is due to tetrahydrobiopterin deficiency. Biochem J 2000; **349:** 353–356.

26 Du XL, Edelstein D, Dimmeler S, Ju Q, Sui C, Brownlee M. Hyperglycemia inhibits endothelial nitric oxide synthase activity by posttranslational modification at the Akt site. J Clin Invest 2001; **108:** 1341–1348.

27 Shinozaki K, Nishio Y, Okamura T *et al.* Oral administration of tetrahydrobiopterin prevents endothelial dysfunction and vascular oxidative stress in the aortas of insulin-resistant rats. Circ Res 2000; **87:** 566–573.

28 Laursen JB, Somers M, Kurz S *et al.* Endothelial regulation of vasomotion in apoE-deficient mice: implications for interactions between peroxynitrite and tetrahydrobiopterin. Circulation 2001; **103:** 1282–1288.

29 Ni W, Egashira K, Kataoka C *et al.* Antiinflammatory and antiarteriosclerotic actions of HMG-CoA reductase inhibitors in a rat model of chronic inhibition of nitric oxide synthesis. Circ Res 2001; **31:** 415–421.

30 Adler AI, Stratton IM, Neil HA *et al.* Association of systolic blood pressure with macro-vascular and microvascular complications of type 2 diabetes prospective observational study. BMJ 2000; **321:** 412–419.

31 Pyorala K, Pedersen TR, Kjekshus J, Faergeman O, Olsson AG, Thorgeirsson G. Cholesterol lowering with simvastatin improves prognosis of diabetic patients with coronary heart disease. A subgroup analysis of the Scandinavian Simvastatin Survival Study (4S). Diabetes Care 1997; **20:** 614–620.

32 Simons JM, Hart BA, Ip Vai Ching TRA, Van Dijk H, Labadie RP. Metabolic activation of natural phenols into selective oxidative burst agonists by activated human neutrophils. Free Radic Biol Med 1990; **8:** 251–258.

33 Gajewska G, Ganowiak Z, Grzybowski J, Radecki A, Wrzesniowska K. Analysis of an industrial smoke

